A reduced polytopic LPV synthesis for a sampling varying controller : experimentation with a T inverted pendulum

David Robert, Olivier Sename and Daniel Simon

Abstract— This paper deals with the adaptation of a real-time controller's sampling period to account for the available computing resource variations. The design of such controllers requires a parameter-dependent discrete-time model of the plant, where the parameter is the sampling period. A polytopic approach for LPV (Linear Parameter Varying) systems is then developed to get an H_∞ sampling period dependent controller. A reduction of the polytope size is here performed which drastically reduces the conservatism of the approach and makes easier the controller implementation. Some experimental results on a T inverted pendulum are provided to show the efficiency of the approach.

Index Terms— Digital control, linear parameter varying systems, H_∞ control, real experiments.

I. INTRODUCTION

High-technology applications (cars, household appliances..) are using more and more computing and network resources, leading to a need of consumption optimisation for decreasing the cost or enhancing reliability and performances. A solution is to improve the flexibility of the system by on-line adaptation of the processor/network utilisation, either by changing the algorithm or by adapting the sampling period. This paper deals with the latter case and presents the synthesis of a control law with varying sampling period.

Few recent works have been devoted to the computing resource variations. In [1] a feedback controller with a sampling period dependent PID controller is used. In [2], [3] a feedback scheduler based on a LQ optimisation of the control tasks periods is proposed. In [4] a processor load regulation is proposed and applied for real-time control of a robot arm. In [5] the design of a sampling period dependent RST controller was proposed.

The presented contribution enhances a previous paper ([6]) using a linear parameter-varying (LPV) approach of the robust linear control framework. The main point is the problem formulation such that it can be solved following the LPV design of [7]. We first propose a parametrised discretization of the continuous time plant and of the weighting functions, leading to a discrete-time sampling period dependent augmented plant. In particular the plant discretization approximates the exponential by a Taylor series of

order N. Therefore the LPV design we formerly used build discrete-time sampling period dependent controller through the convex combination of 2^N controllers, which may be conservative and complex to implement. In this paper we exploit the dependency between the variables parameters, which are the successive powers of the sampling period $h, h^2, ..., h^N$, to reduce the number of controllers to be combined to $N + 1$. This reduction of the polytopic set drastically decreases the conservatism of the previous work and makes the solution easier to implement. This approach is then validated by experiments on real-time control of a T inverted pendulum.

The outline of this paper is as follows. Section II describes the plant discretization and the reduction of the original complexity using the parameters dependency. In section III the closed-loop objectives are stated and expressed as weighting functions in the H_∞ framework. Section IV comments briefly the augmented plant and gives background on H_∞/LPV control design. The experiments on the T inverted pendulum are described in section V. Finally, the paper ends with some conclusions and further research directions.

II. A POLYTOPIC DISCRETE-PLANT MODEL

We consider a state space representation of continuous time plants as :

$$G : \begin{cases} \dot{x} &= Ax + Bu \\ y &= Cx + Du \end{cases} \qquad (1)$$

The exact discretization of this system with a zero order hold at the sampling period h can be computed using expression (2) and (3), see [8].

$$\begin{pmatrix} A_d & B_d \\ 0 & I \end{pmatrix} = exp(\begin{pmatrix} A & B \\ 0 & 0 \end{pmatrix} h) \qquad (2)$$

$$C_d = C \qquad D_d = D \qquad (3)$$

This leads to the discrete-time LPV system (4)

$$G_d : \begin{cases} x_{k+1} &= A_d(h) x_k + B_d(h) u_k \\ y_k &= C_d(h) x_k + D_d(h) u_k \end{cases} \qquad (4)$$

with h ranging in $[h_{min}; h_{max}]$. However in (2) A_d and B_d are not affine on h.

A. Preliminary approach: Taylor expansion

To get a polytopic model (and then apply an LPV design), we propose to approximate the exponential by a Taylor series of order N as :

$$e^{Mh} \approx \sum_{i=0}^{N} \frac{(Mh)^i}{i!}, \qquad (5)$$

which leads, with $H = [h \ h^2 \ \dots \ h^N]$, to

$$A_d(h) \approx I + \sum_{i=1}^{N} \frac{A^i}{i!} h^i := A_d(H) \qquad (6)$$

$$B_d(h) \approx \sum_{i=1}^{N} \frac{A^{i-1}B}{i!} h^i := B_d(H) \qquad (7)$$

Now the dependence on H is affine. To get a polytope $\mathscr{H}$ containing H, a solution is to choose $\mathscr{H}$ with the 2^N vertices ω_i corresponding to the vertices of the hypercube (9).

$$\mathscr{H} = \left\{ \sum_{i=1}^{2^N} \alpha_i(h)\omega_i : \alpha_i(h) \geq 0, \sum_{i=1}^{2^N} \alpha_i(h) = 1 \right\} \qquad (8)$$

$$\{h, h^2, \dots, h^N\}, \ h^i \in \{h_{min}^i, h_{max}^i\} \qquad (9)$$

This leads to the plant polytopic model (10) where G_{d_i} are $G_d(H)$ evaluated at the vertices ω_i.

$$G_d(H) = \sum_{i=1}^{2^N} \alpha_i(h)G_{d_i} \quad \text{and} \quad H = \sum_{i=1}^{2^N} \alpha_i(h)\omega_i \qquad (10)$$

As the gain-scheduled controller will be a convex combination of 2^N "vertex" controllers, the choice of the series order N gives a trade-off between the approximation accuracy and the controller complexity. To reduce the complexity (and the conservatism of the corresponding control design as well), a reduction of the polytope is proposed in the next section.

B. Reduction of the polytope

In (6), h, h^2, ..., h^N are viewed as independent parameters which leads to some conservatism and useless complexity. To decrease the volume and number of vertices of the matrices polytope we now exploit the dependency between the successive powers of the parameter h.

The parameter range $0 \leq h_{min} \leq h \leq h_{max}$ with $0 < h_{max}$ leads to :

$$h^{n+1} \leq h^n \ h_{max} \qquad (11)$$

Recall that the vertices ω_i of $\mathscr{H}$ are defined by $h, h^2, \dots, h^N$ with $h^i \in \{h_{min}^i, h_{max}^i\}$. Considering the constraint (11) leads to the following set of admissible vertices :

$$\omega_1 = [h_{min}, h_{min}^2, h_{min}^3, \dots, h_{min}^N]$$
$$\omega_2 = [h_{\mathbf{max}}, h_{min}^2, h_{min}^3, \dots, h_{min}^N]$$
$$\omega_3 = [h_{\mathbf{max}}, h_{\mathbf{max}}^2, h_{min}^3, \dots, h_{min}^N] \qquad (12)$$
$$\vdots$$
$$\omega_{N+1} = [h_{\mathbf{max}}, h_{\mathbf{max}}^2, h_{\mathbf{max}}^3, \dots, h_{\mathbf{max}}^N]$$

Therefore we get $N+1$ vertices rather than 2^N. Note that these vertices are linearly independent and make a simplex, which is itself basically a polytope [9].

When $N = 2$ the square is downsized to the triangle in figure 1. When $N = 3$ the pyramid in figure 2 is the reduction of a cube.

Remark 1: Note that exact calculations of matrix exponential via diagonalising or Cayley-Hamilton theorems are
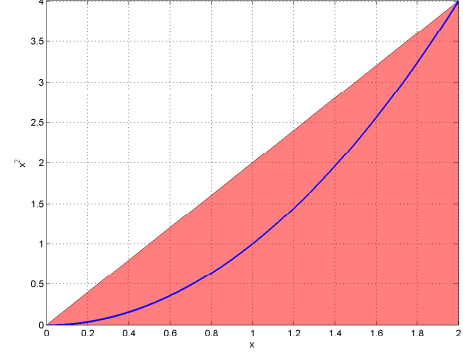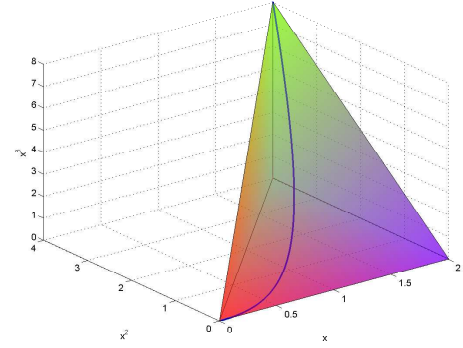

Fig. 1.   Polytope reduction for N=2

Fig. 2.   Polytope reduction for N=3

more involved here as their expression will lead to non affine representations of $A_d(H)$ and $B_d(H)$.

Remark 2: Taylor's approximation, especially of low order, is inaccurate for large value of the parameter h. Therefore it is important to split (5) as $e^{Mh} = e^{M(h_0+\delta_h)} = e^{Mh_0}e^{M\delta_h}$ with $\delta_h \in [h_0 - h_{min}; h_{max} - h_0]$, then calculate exactly e^{Mh_0} and apply approximation only on $e^{M\delta_h}$ (see section V).

To evaluate the approximation error due to the Taylor approximation (in both cases of full and reduced polytope), the criterion (13) is used. The H_∞ norm is chosen here to express the worst case error between G_{d_e} and G_d, two discretizations which use matrix exponential and Taylor series approximation of order N respectively.

$$J_N = \max_{h_{min} < h < h_{max}} \| G_{d_e}(h, z) - G_d(h, z) \|_\infty \qquad (13)$$

III. PERFORMANCE SPECIFICATION

In the H_∞ framework, the general control configuration of figure 3 is considered, where W_i and W_o are weighting functions specifying closed-loop performances (see [10]). The objective is here to find a controller K such internal stability is achieved and $\|\tilde{z}\|_2 < \gamma\|\tilde{w}\|_2$, where γ represents the H_∞ attenuation level.

Classical control design assumes constant performance objectives and produces a controller with an unique sampling period. This sampling period is chosen according to the
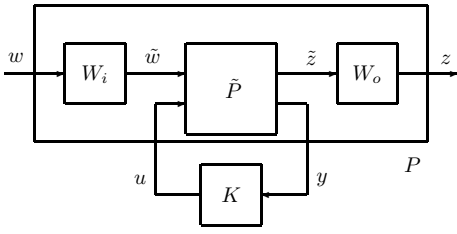
Fig. 3. Focused interconnection

controller bandwidth, the noise sensibility and the availability of computation resources. When the sampling period varies the usable controller bandwidth also varies and the closed-loop objectives should logically be adapted ; therefore we propose to adapt the bandwidth of the weighting functions. In this aim, W_i and W_o are split into two parts :

- a constant part with constant poles and zeros. This allows, for instance, to compensate for oscillations or flexible modes which are, by definition, independent of the sampling period. This part is merged with the plant before its discretization.
- the variable part contains poles and zeros whose pulsations are expressed as an affine function of the frequency $f = 1/h$. This permits to adapt the bandwidth of the weighting functions. These poles and zeros are here constrained to be *real* by the discretization step.

To discretize the variable part $V(s)$ of a weighting function, we propose the following methodology

1) factorise $V(s)$ as a product of first order systems, with $a_i, b_i \in \mathbb{R}$

$$V(s) = \beta \prod_i \frac{s - b_i f}{s - a_i f} = \beta \prod_i V_i(s) \qquad (14)$$

2) use the observable canonical form for $V_i(s)$

$$V_i(s) : \begin{cases} \dot{x}_i = a_i f \ x_i + f(a_i - b_i) \ u_i \\ y_i = x_i + u_i \end{cases} \qquad (15)$$

3) form the series interconnection of the state space representation of each $V_i(s)$ and thus

$$V(s) : \begin{cases} \dot{x}_v = A_v f \ x_v + B_v f \beta u_v \\ y_v = C_v \ x_v + D_v \beta u_v \end{cases} \qquad (16)$$

4) discretize the state space representation of $V(s)$. Thanks to the affine dependence in f in (16) the discrete-time model of the variable part becomes independent of h since:

$$\begin{cases} A_{v_d} = e^{A_v f h} = e^{A_v} \\ B_{v_d} = (A_v f)^{-1}(A_{v_d} - I)\beta B_v f = A_v^{-1}(A_{v_d} - I)\beta B_v \\ C_{v_d} = C_v \text{ and } D_{v_d} = D_v \end{cases} \qquad (17)$$

Remark 3: The serial interconnection of two systems $V_i(s)$ leads to the expressions (18). It is easy to verify that even with more than two first order systems, matrices A and B of

$V(s)$ remain affine in f :

$$A_v = \begin{pmatrix} a_1 & 0 \\ a_2 - b_2 & a_2 \end{pmatrix} \qquad B_v = \begin{pmatrix} a_1 - b_1 \\ a_2 - b_2 \end{pmatrix}$$

$$C_v = \begin{pmatrix} 1 & 1 \end{pmatrix} \qquad D_v = 1 \qquad (18)$$

$$x_v = (x_1 \ x_2)^T$$

Remark 4: The simplification between f and h in (17) makes easy the discretization step. This is why plant and weighting functions are separately discretized and the augmented plant is obtained in discrete time afterwards by interconnection.

IV. LPV/H_∞ CONTROL DESIGN

Interconnection of figure 3 between the discrete-time polytopic model of the plant $\tilde{P}$ (A, B_w, B_u, C_z, C_y, D_{zw}, D_{zu}, D_{yw}, D_{yu}) and the weighting functions W_i (A_i, B_i, C_i, D_i) and W_o (A_o, B_o, C_o, D_o) leads to the discrete-time LPV augmented plant $P(H)$,

$$P(H) = \begin{pmatrix} A(H) & B_w(H)C_i & 0 & B_w(H) & B_u(H) \\ 0 & A_i & 0 & B_i & 0 \\ B_oC_z & B_oD_{zw}C_i & A_o & B_oD_{zw}D_i & B_oD_{zu} \\ \hline D_oC_z & D_oD_{zw}C_i & C_o & D_oD_{zw}D_i & D_oD_{zu} \\ C_y & D_{yw}C_i & 0 & D_{yw}D_i & D_{yu} \end{pmatrix}$$

with $H \in \mathscr{H}$ \qquad (19)

$$:= \begin{pmatrix} \bar{A}(H) & \bar{B}_1(H) & \bar{B}_2(H) \\ \hline \bar{C}_1(H) & \bar{D}_{11}(H) & \bar{D}_{12}(H) \\ \hline \bar{C}_2(H) & \bar{D}_{21}(H) & \bar{D}_{22}(H) \end{pmatrix} \qquad (20)$$

We aim to use here the H_∞ control design for linear parameter-varying systems as stated in [7]. Let the discrete-time LPV plant, mapping exogenous inputs w and control inputs u to controlled outputs z and measured outputs y, with $x \in \mathbb{R}^n$, be given by the polytopic model

$$\begin{cases} x_{k+1} = \bar{A}(H)x_k + \bar{B}_1(H)w + \bar{B}_2(H)u \\ z = \bar{C}_1(H)x_k + \bar{D}_{11}(H)w + \bar{D}_{12}(H)u \\ y = \bar{C}_2(H)x_k + \bar{D}_{21}(H)w + \bar{D}_{22}(H)u \end{cases} \qquad (21)$$

where the dependence of $A(H)$, $B(H)$, $C(H)$ and $D(H)$ on H is affine and the parameter vector H, ranges over a fixed polytope $\mathscr{H}$ with r vertices ω_i

$$\mathscr{H} = \left\{ \sum_{i=1}^r \alpha_i(h)\omega_i : \alpha_i(h) \geq 0, \sum_{i=1}^r \alpha_i(h) = 1 \right\} \qquad (22)$$

where r is equal to $N+1$ or to 2^N according to the kind of polytope (reduced or full).

Proposition 1: Under the assumptions :

(A1) $\bar{D}_{22}(H) = 0$

(A2) $\bar{B}_2(H), \bar{C}_2(H), \bar{D}_{12}(H), \bar{D}_{21}(H)$ are parameter- independent

(A3) the pairs $(\bar{A}(H), \bar{B}_2)$ and $(\bar{A}(H), \bar{C}_2)$ are quadratically stabilizable and detectable over H respectively,

the gain-scheduled controller

$$\begin{cases} x_{K_{k+1}} = A_K(H)x_{K_k} + B_K(H)y_k \\ u_k = C_K(H)x_{K_k} + D_K(H)y_k \end{cases} \qquad (23)$$

where $x_K \in \mathbb{R}^n$, ensures over all parameter trajectories, for the closed-loop system of figure (4):
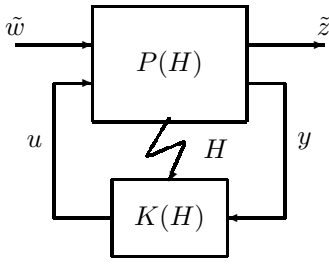
Fig. 4.   Closed-loop of the LPV system

- closed-loop quadratic stability
- $\mathscr{L}_2$-induced norm of the operator mapping w into z bounded by γ, i.e. $\|z\|_2 < \gamma \|w\|_2$

if and only if there exist γ and two symmetric matrices (R, S) satisfying $2r + 1$ LMIs (which are computed off-line) :

$$\left(\frac{N_R \mid 0}{0 \mid I} \right)^T \mathscr{L}_1 \left(\frac{N_R \mid 0}{0 \mid I} \right) < 0, i = 1 \ldots r \qquad (24)$$

$$\left(\frac{N_S \mid 0}{0 \mid I} \right)^T \mathscr{L}_2 \left(\frac{N_S \mid 0}{0 \mid I} \right) < 0, i = 1 \ldots r \qquad (25)$$

$$\begin{pmatrix} R & I \\ I & S \end{pmatrix} \geq 0 \qquad (26)$$

where

$$\mathscr{L}_1 = \left(\begin{array}{cc|c} \bar{A}_i R \bar{A}_i^T - R & \bar{A}_i R \bar{C}_{1i}^T & \bar{B}_{1i} \\ \bar{C}_{1i} R \bar{A}_i^T & -\gamma I + \bar{C}_{1i} R \bar{C}_{1i}^T & \bar{D}_{11i} \\ \hline \bar{B}_{1i}^T & \bar{D}_{11i}^T & -\gamma I \end{array} \right)$$

$$\mathscr{L}_2 = \left(\begin{array}{cc|c} \bar{A}_i^T S \bar{A}_i - S & \bar{A}_i^T S \bar{B}_{1i} & \bar{C}_{1i}^T \\ \bar{B}_{1i}^T S \bar{A}_i & -\gamma I + \bar{B}_{1i}^T S \bar{B}_{1i} & \bar{D}_{11i}^T \\ \hline \bar{C}_{1i} & \bar{D}_{11i} & -\gamma I \end{array} \right)$$

$\bar{A}_i$, $\bar{B}_{1i}$, $\bar{C}_{1i}$, $\bar{D}_{11i}$ are $\bar{A}(H)$, $\bar{B}_1(H)$, $\bar{C}_1(H)$, $\bar{D}_{11}(H)$ evaluated at the ith vertex of the parameter polytope. N_S and N_R denote bases of null spaces of $(\bar{B}_2^T, \bar{D}_{12}^T)$ and $(\bar{C}_2, \bar{D}_{21})$ respectively.

Once R, S and γ are obtained, the controllers are reconstructed at each vertex of the parameter polytope. The gain-scheduled controller $K(H)$ is then the convex combination of these controllers

$$K(H) : \begin{pmatrix} A_K(H) & B_K(H) \\ C_K(H) & D_K(H) \end{pmatrix} = \sum_{i=1}^{r} \alpha_i(h) \begin{pmatrix} A_{K_i} & B_{K_i} \\ C_{K_i} & D_{K_i} \end{pmatrix} \quad (27)$$

$$\text{with } \alpha_i(h) \text{ such that } H = \sum_{i=1}^{r} \alpha_i(h) \omega_i \qquad (28)$$

Remark 5: This synthesis uses a constant Lyapunov function approach which is known to produce a sub-optimal controller.

Remark 6: In (19) assumption (A2) is not satisfied due to $B_u(H)$ term in $B_2(H)$. To avoid this, a strictly proper filter is added on the control input. It is a numerical artifact, therefore its bandwidth should be chosen high enough to be negligible regarding the plant and objective bandwidths.

Note that on-line scheduling of the controller needs the computation of $\alpha_i(h)$ knowing h which is easy with the reduced polytope $\mathscr{H}$ ([11], [12]). These polytopic coordinates are solutions of the following system :

$$\begin{cases} \sum_{i=1}^{N+1} \alpha_i(h) \omega_i = H = [h, h^2, ..., h^N] \\ \sum_{i=1}^{N+1} \alpha_i(h) = 1, \ \alpha_i(h) \geq 0 \end{cases} \qquad (29)$$

which leads, for the case $N = 2$ of the next section to the simple explicit solutions:

$$\alpha_1 = \frac{h_{max} - h}{h_{max} - h_{min}}, \alpha_2 = 1 - (\alpha_1 + \alpha_3), \alpha_3 = \frac{h^2 - h_{min}^2}{h_{max}^2 - h_{min}^2}$$

V. CONTROL OF THE T INVERTED PENDULUM

This section is devoted to an experimental validation of the approach using a "T" inverted pendulum of Educational Control Products[1], available at LAG, in the NeCS (Network Controlled Systems) project. These experiments will emphasise the applicability of the proposed design method.

A. System description

The pendulum is shown in figure 5.

The pendulum scheme in figure 6 is composed of two rods. A vertical one which rotates around the pivot axle, and an horizontal sliding balance one. Two optional masses allow to modify the plan dynamical behaviour.

The control actuator (DC motor) delivers a force u to the horizontal sliding rod, through a drive gear-rack.

The θ angle, positive in the trigonometric sense, is measured by the rod angle sensor. The position z of the horizontal rod is measured by a sensor located at the motor axle.

The DC motor is torque controlled using a local current feedback loop (assumed to be a simple gain due to the high dynamics). The dynamical behaviour of the sensors is also neglected.

B. Modelling

A mechanical model of the pendulum is presented below, which takes into account the viscous friction (but not the Coulomb friction).

$$\begin{pmatrix} m_1 & m_1 l_0 \\ m_1 l_0 & \bar{J} \end{pmatrix} \begin{pmatrix} \ddot{z} \\ \ddot{\theta} \end{pmatrix} + \begin{pmatrix} -f_{v_z} & -m_1 z \dot{\theta} \\ 2 m_1 z \dot{\theta} & 0 \end{pmatrix} \begin{pmatrix} \dot{z} \\ \dot{\theta} \end{pmatrix}$$
$$+ \begin{pmatrix} -m_1 \sin \theta \\ -(m_1 l_0 + m_2 l_c) \sin \theta - m_1 z \cos \theta \end{pmatrix} g = \begin{pmatrix} u \\ 0 \end{pmatrix} \quad (30)$$

where the time dependence of the state variables is implicit, and the parameter values of given below in table I.

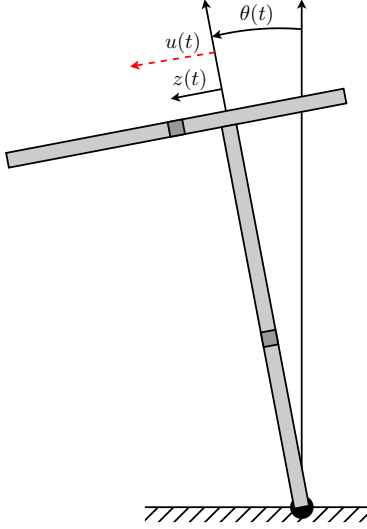[1]http://www.ecpsystems.com/controls_pendulum.htm

Fig. 5.   Picture of the T pendulum

Fig. 6.   Coordinates of the T pendulum

TABLE I

PARAMETERS

Name	Value	Description
m_1	0.217 kg	horizontal sliding rod mass
m_2	1.795 kg	vertical rod mass
l_0	0.33	vertical rod length
l_c	-0.032 m	vertical rod position of the centre of gravity
g	9.81 m.s^{-2}	gravity acceleration
$\bar{J}$	0.061 Nm^2	Nominal inertia
f_{v_z}	0.1 kg.s^{-1}	viscous friction

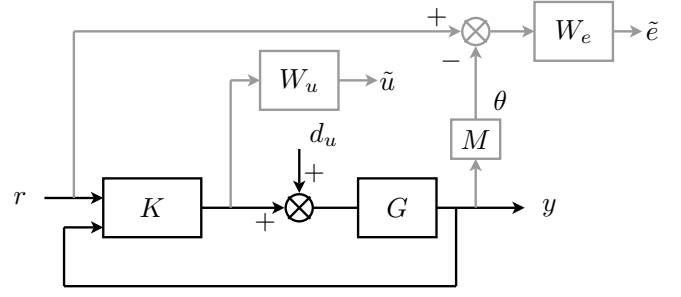Choosing the state vector as $x = [z, \dot{z}, \theta, \dot{\theta}]$, we get the

Fig. 7.   General control configuration

following non linear state space representation:

$$\begin{cases}
\dot{x}_1 = x_2 \\
\dot{x}_2 = -l_0\dot{x}_4 + x_1 x_4^2 + g\sin x_3 - \dfrac{f_{v_z}}{m_1}x_2 + \dfrac{u}{m_1} \\
\dot{x}_3 = x_4 \\
\dot{x}_4 = \dfrac{1}{J_0(x_1) - m_1 l_0^2}(+g(m_1 x_1 \cos x_3 + m_2 l_c \sin x_3) \\
\qquad\quad -m_1(l_0 x_4 + 2x_2)x_1 x_4 - l_0 u)
\end{cases} \quad (31)$$

with $J_0(x_1) = \bar{J} + m_1 x_1^2$. The steady-state linearisation around $x = [0,0,0,0]$ gives the linear state space representation $\dot{x}(t) = Ax(t) + Bu(t)$, $y(t) = Cx(t)$ with

$$A = \begin{pmatrix} 0 & 1 & 0 & 0 \\ \frac{-l_0 g m_1}{\bar{J}-m_1 l_0^2} & -\frac{f_{v_z}}{m_1} & \frac{-l_0 g m_2 l_c}{\bar{J}-m_1 l_0^2}+g & 0 \\ 0 & 0 & 0 & 1 \\ \frac{g m_1}{\bar{J}-m_1 l_0} & 0 & \frac{g m_2 l_c}{\bar{J}-m_1 l_0^2} & 0 \end{pmatrix}, B = \begin{pmatrix} 0 \\ \frac{l_0^2}{\bar{J}-m_1 l_0^2}+\frac{1}{m_1} \\ 0 \\ \frac{-l_0}{\bar{J}-m_1 l_0^2} \end{pmatrix}$$

$$C = \begin{pmatrix} 1 & 0 & 0 & 0 \\ 0 & 0 & 1 & 0 \end{pmatrix}$$

which gives numerically:

$$A = \begin{pmatrix} 0 & 1 & 0 & 0 \\ -18.79 & -0.46 & 14.82 & 0 \\ 0 & 0 & 0 & 1 \\ 56.92 & 0 & -15.18 & 0 \end{pmatrix} \quad B = \begin{pmatrix} 0 \\ 7.52 \\ 0 \\ -8.82 \end{pmatrix} \quad (32)$$

The poles of the linear model are $p_{1,2} = -0.122 \pm 6.784$, $p_3 = -3.592$ and $p_4 = 3.376$.

C. Performance specification

As such a T pendulum system is difficult to be controlled, our main objective is here to get a closed-loop stable system, to emphasise the practical feasibility of the proposed methodology for real-time control.

The sampling period is assumed to be in the interval $[1,3]$ *ms*.

The chosen performance objectives are represented in figure 7, where the tracking error and the control input are weighted (as usual in the H_∞ methodology).

This corresponds to the mixed sensitivity problem given in (33).

$$\left\| \begin{matrix} W_e(I - MS_y GK_1) & W_e MS_y G \\ W_u S_u K_1 & W_u T_u \end{matrix} \right\|_\infty \leq \gamma \quad (33)$$
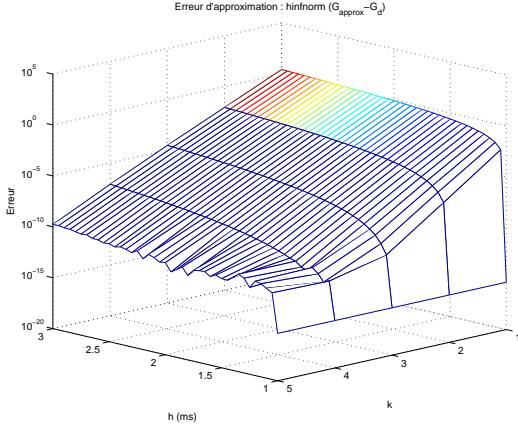
Fig. 8. Approximation error

with

$$K = \begin{bmatrix} K_1 & K_2 \end{bmatrix} \qquad M = \begin{bmatrix} 0 & 0 & 1 & 0 \end{bmatrix}$$
$$S_u = (I - K_2 G)^{-1} \qquad S_y = (I - G K_2)^{-1}$$
$$T_u = -K_2 G (I - K_2 G)^{-1} \qquad (34)$$

The performance objectives are represented by weighting functions and may be given by the usual transfer functions [10]:

$$W_e(p,f) = \frac{p M_S + \omega_S(f)}{p + \omega_S \varepsilon_S} \qquad \omega_S(f) = h_{min} \, \omega_{S_{max}} f \quad (35)$$

$$W_u(p,f) = \frac{1}{M_U} \qquad (36)$$

where $f = 1/h$, $\omega_{S_{max}} = 1,5$ rad/s, $M_S = 2$, $\varepsilon_S = 0.01$ and $M_U = 5$.

D. Polytopic discrete-time model

We follow here the methodology proposed in section II. The approximation is done around the nominal period $h_o = 1ms$, for $h \in [1,3]$ ms, i.e. $\delta_h \in [0,2]$ ms (see Remark 2).

On figure 8 the criterion (13) is evaluated for different sampling periods ($h \in [1,3]ms$) and different orders of the Taylor expansions ($k \in [1,5]$). It shows that this error may be large if the order 1 is used.

On figure 9 $|G_{d_e}(\delta_h,z) - G_d(\delta_h,z)|$ is plotted according to the frequency, evaluated for 5 sampling periods (i.e. $\delta_h \in [0,2]ms$) and for two cases of Taylor expansions (2 and 4). This allows to conclude that the choice of an order 2 of the Taylor expansion is quite good as it leads to an approximation error less than $-40dB$.

Note that choosing the case "order 2" leads to a reduced polytope with 3 vertices.

E. LPV/H_∞ design

The first step is the discretization of the weighting functions. The augmented system is got, using a preliminary filtering of the control input, to satisfy the design assumptions. The augmented system is of order 6.
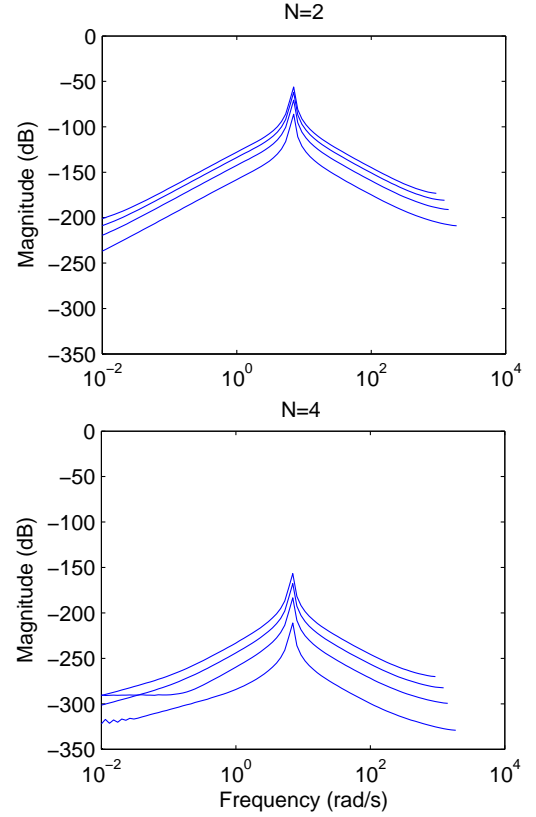Applying the design method developed in section IV leads to

Fig. 9. $|G_{d_e}(\delta_h,z) - G_d(\delta_h,z)|$ for $\neq h$ - Taylor order 2 and 4

the following results, combining the Taylor expansion order and the polytope reduction:

	Polytope	Nb vertices	γ_{opt}
Taylor order N=2	full	4	1.1304
Taylor order N=2	reduced	3	1.1299
Taylor order N=4	full	16	1.1313
Taylor order N=4	reduced	5	1.1303

This table emphasises that both design of orders 2 and 4 are reliable. For implementation reasons (simplicity and computational complexity) we have chosen the case of the reduced polytope using a Taylor expansion of order 2.

The corresponding sensitivity functions of the above design are shown in figure 10. Using $S_e = e/r$ the steady-state tracking error is less than $-46dB$, with a varying bandwidth from 0.4 to 1.2 rad/s, i.e the ratio 3, specified according to the interval of sampling period is satisfied.

The peak value of $S_u K_1$ varies from 1.2 to 10.8dB, which is reasonable for the control gain. Note that we will benefit from the relatively high sensitivity in high frequencies, because it allows some persistence noise in the control action, allowing to reduce the effect of friction, as we will see in the experiments.

Finally the function $M S_y G d_u$ is very low so that the effect of input disturbance d_u on the tracking error will be greatly attenuated.

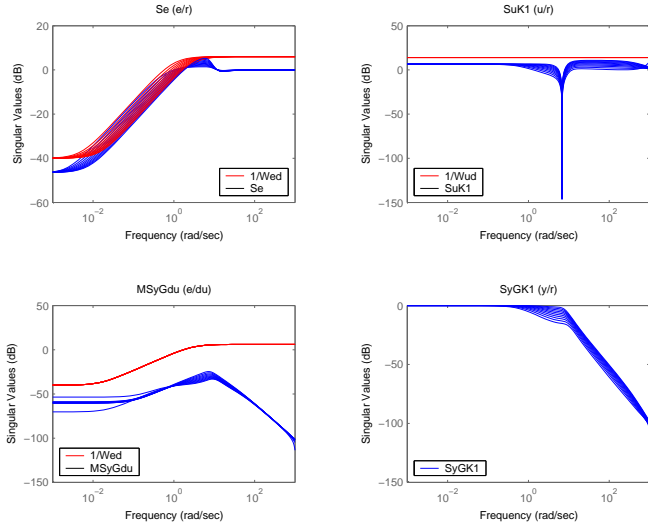On figure 11 the time-domain response of the non linear pendulum model (angle and position) interconnected with

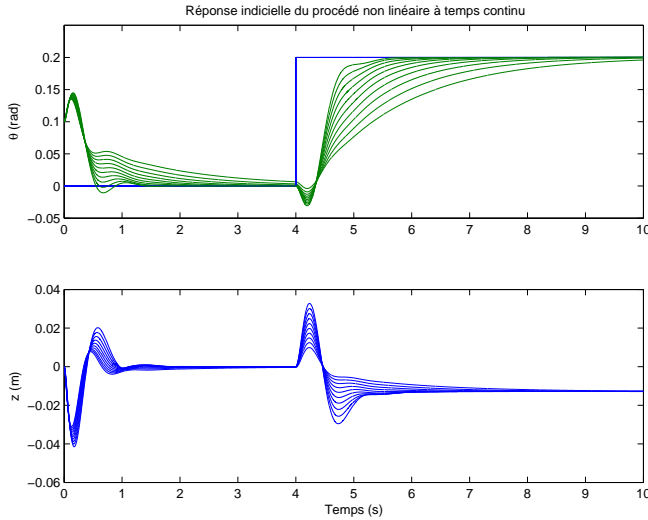Fig. 10.   Sensitivity functions

Fig. 12.   Motion of the T pendulum under a sinusoidal sampling period

Fig. 11.   Response time of the continuous time non-linear process

Fig. 13.   Motion of the T pendulum under a square sampling period

the discrete-time LPV sampling variable controller (here for different frozen values of the sampling periods) is shown. The settling time varies from 1.1 to 4.8 sec, i.e. in a ratio 4.3 with is very interesting for real-time control. There is no overshoot as seen on the frequency responses of the sensitivity function S_yGK_1.

F. Simulation results

In this section, the application of the proposed sampling variable controller when the sampling period varies between 1 and 3 msec. is provided.

Two cases are presented. First in figure 12 the sampling period variation is continuous and follows a sinusoidal signal of frequency $0.15 rad/s$. Then in figure 13 some step changes of the sampling period are done.

These results show that the settling time of the closed-loop system varies according to the sampling period, as expected. When the period is large (i.e for $t = 10 sec$) the pendulum is

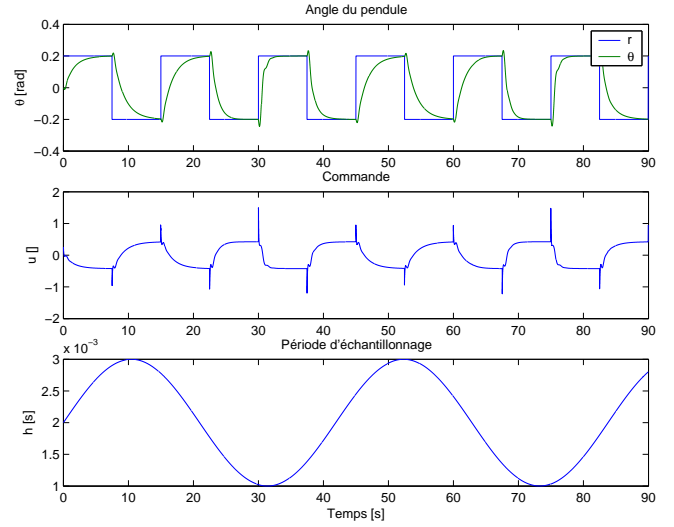slower, while when the period is large (i.e for $t = 30 sec$ in Fig. 12) the pendulum response is faster. Moreover, thanks to the LPV approach, the variations (sinusoidal or step changes) of the sampling period do not lead to abrupt transient of the pendulum behaviour. This is a great benefit of the LPV approach which ensures the stability evens for quick variations of the parameter (this is due to the use of a single Lyapunov function in the design [7]). The same assessment can be done for the control input.

The LPV scheme allows here to guarantee the closed-loop quadratic stability, a bounded $\mathscr{L}_2$-induced norm for all variation of the sampling period and have a predictable closed-loop behaviour.

G. Experiments

The same scenarii as the previous section (simulation results) are now implemented for the real plant of figure 5.
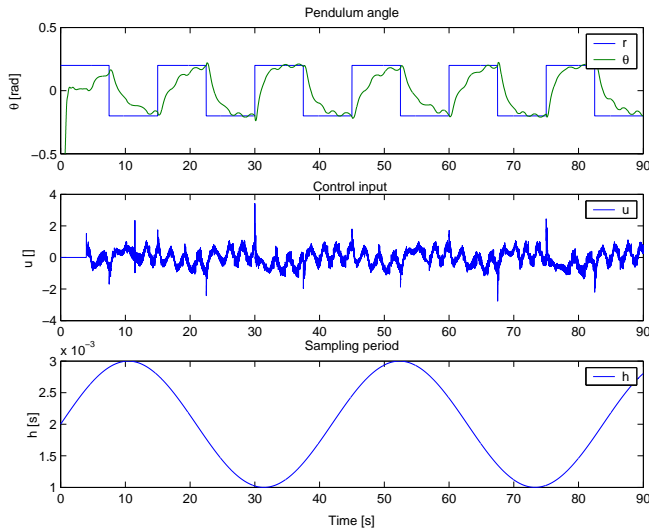
Fig. 14. Experimental motion of the T pendulum under a sinusoidal sampling period
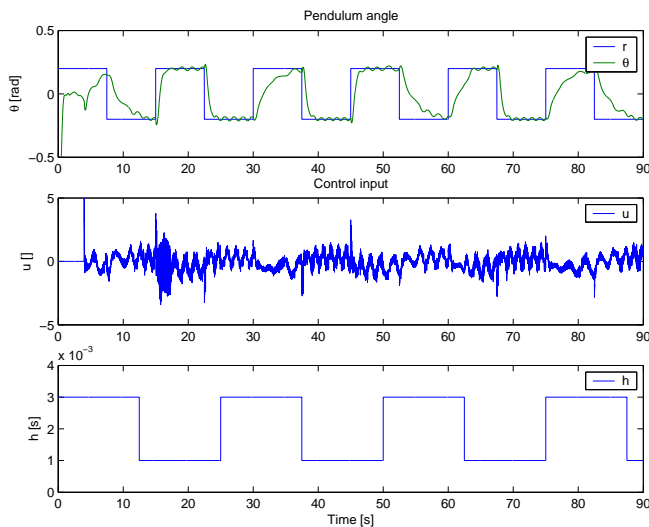

Fig. 15. Experimental motion of the T pendulum under a square sampling period

This plant is controlled through Matlab/Simulink using the Real-time Workshop and xPC Target.

The results are given in figures 14 and 15. As in the previous section, the settling time is minimal when the sampling period is maximal, and vice versa. In the same way, there is no abrupt changes in the control input (even when the sampling period vary from 1 to 3 ms as in figure 15).

Note that, as explained before, the real control input is sensitive to noise, allowing to minimise the friction effect, and therefore to obtain a closed-loop system with much less oscillations.

These results emphasise the great advantage and flexibility of the method when the available computing resources may vary, and when sampling period variations are used to handle such a computing flexibility as in [4].

VI. CONCLUSION

In this paper, an LPV approach is proposed to design a discrete-time linear controller with a varying sampling period and varying performances. Compared to our previous result in [6], a way to reduce the polytope from 2^N to $N+1$ vertices (where N is the Taylor order expansion) is provided, which drastically reduces the conservatism of the results and makes the solution easier to implement.

Also the complete methodology is applied to the case of a "T" inverted pendulum, where experimental results have been given. These results emphasise the real applicability of the LPV approach as well as its interest in the context of adaptation to varying processor or network load where a bank of switching controllers would need too much resources. In our case, the stability and performance property of the closed-loop system are guaranteed whatever the speed of variations of the sampling period are.

REFERENCES

[1] A. Cervin and J. Eker, "Feedback scheduling of control tasks," in *Proceedings of the 39th IEEE Conference on Decision and Control*, Sydney, Australia, Dec. 2000.

[2] A. Cervin, J. Eker, B. Bernhardsson, and K. Årzén, "Feedback-feedforward scheduling of control tasks," *Real-Time Systems*, vol. 23, no. 1–2, pp. 25–53, July 2002.

[3] J. Eker, P. Hagander, and K. Årzén, "A feedback scheduler for real-time controller tasks," *Control Engineering Practice*, vol. 8, no. 12, pp. 1369–1378, Dec. 2000.

[4] D. Simon, D. Robert, and O. Sename, "Robust control/scheduling co-design: application to robot control," in *RTAS'05 IEEE Real-Time and Embedded Technology and Applications Symposium*, San Francisco, march 2005.

[5] D. Robert, O. Sename, and D. Simon, "Sampling period dependent RST controller used in control/scheduling co-design," in *Proceedings of the 16th IFAC World Congress*, Prague, Czech Republic, July 2005.

[6] ——, "Synthesis of a sampling period dependent controller using lpv approach," in *5th IFAC Symposium on Robust Control Design ROCOND'06*, Toulouse, France, july 2006.

[7] P. Apkarian, P. Gahinet, and G. Becker, "Self-scheduled H_∞ control of linear parameter-varying systems: A design example," *Automatica*, vol. 31, no. 9, pp. 1251–1262, 1995.

[8] K. Åström and B. Wittenmark, *Computer-Controlled Systems*, 3rd ed., ser. Information and systems sciences series. New Jersey: Prentice Hall, 1997.

[9] S. Boyd and L. Vandenberghe, *Convex Optimization*. Cambridge University Press, 2004.

[10] S. Skogestad and I. Postlethwaite, *Multivariable Feedback Control: analysis and design*. John Wiley and Sons, 1996.

[11] J.-M. Biannic, "Commande robuste des systmes paramtres variables," Ph.D. dissertation, ENSAE, Toulouse, France, 1996.

[12] A. Zin, "On robust control of vehicle suspensions with a view to global chassis control," Ph.D. dissertation, INPG - Laboratoire d'Automatique de Grenoble, november 3 2005.